ACS OMEGA

Open Access

http://pubs.acs.org/journal/acsodf

Article

Effects of Proximate Analysis on Coal Ash Fusion Temperatures: An Application of Artificial Neural Network

Moshood Onifade,* Abiodun Ismail Lawal, Samson Oluwaseyi Bada, and Amtenge Penda Shivute

Cite This: *ACS Omega* 2023, 8, 39080−39095

Read Online

ACCESS | Metrics & More | Article Recommendations

ABSTRACT: The temperature at which coal ash melts has a significant impact on the operation of a coal-fired boiler. The coal ash fusion temperature (AFT) is determined by its chemical composition, although the relationship between the two varies. Therefore, it is important to have mathematical models that can reliably predict the coal AFTs when designing coal-based processes based on their coal ash chemistry and proximate analysis. A computational intelligence model based on the interrelationships between coal properties and AFTs was used to predict the AFTs of the coal investigated. A model that integrates the ash, volatile matter, fixed carbon contents, and ash chemistry as input and the AFT [softening temperature, deformation temperature, hemispherical temperature, and flow temperature] as an output provided the best indicators to predict AFTs. The findings from the models indicate (a) a method for determining the AFTs from the coal properties; (b) a reliable technique to calculate the AFTs by varying the proximate analysis; and (c) a better understanding of the impact, significance, and interactions of coal properties regarding the thermal properties of coal ash. This study creates a predictive model that is easy to use, computer-efficient, and highly accurate in predicting coal AFTs based on their ash chemistry and proximate analysis data.

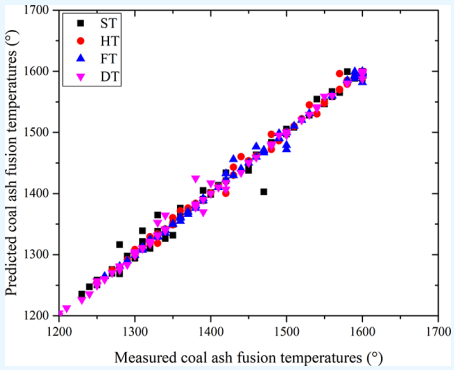

1. INTRODUCTION

Coal is a complex substance consisting mostly of carbon, hydrogen, oxygen, nitrogen, and sulfur, as well as a small quantity of mineral components. The performance index of coal can be preliminarily determined from these components along with a series of analytical tests.[1,2] The electricity, steel, and other industries are extremely concerned with the performance indicators of coal combustion and gasification in the coal resource utilization process.[3,4] The fixed carbon in pulverized coal participates in the chemical reaction during combustion and gasification; the volatile matter (VM) evaporates and disappears during heating; and the mineral composition in the ash changes as well. Because different types of coal contain different mineral components, the presence of specific minerals at elevated temperatures causes the liquid phase to develop early and stick to the surface of the boiler tubes, a phenomenon called "slagging".[5,6]

When designing a boiler to fit a coal or a varied coal range, it is important to take the coal ash fusion properties into account. Regarding the association of coal minerals, the coal ash characterization provides the main mechanism regulating the heating effectiveness of the coal in the pulverized coal-fired boiler.[7] Ash parameters, such as AFTs and ash elemental composition, can be influenced in response to variations in coal qualities, which could result in slagging or fouling problems inside the boiler.[5] The primary cause may be traced to either the low melting point of ash or the high temperature of the combustion process. The majority of coal-fired power plants obtain their coal from various mining operations. In general, the quality of coal varies. Numerous aspects of the economics of power plants are influenced by variations in coal properties such as the ash content and constituents, moisture content, sulfide in flue gas emissions, specific energy, and carbon in fly ash.[8,9]

SiO_2, Al_2O_3, Fe_2O_3, P_2O_5, TiO_2, CaO, MgO, K_2O, Na_2O, and SO_3 are the main chemical components of coal ash[8] and according to previous research, the composition of the coal ash influences the AFTs.[10] Ash typically fuses at higher temperatures when it contains more acid oxides (SiO_2, Al_2O_3, TiO_2, etc.) than when it has more alkaline compositions.[11] Since SiO_2 and Al_2O_3 make up the majority of coal ash, the Si/Al ratio is another important variable that affects the fluidity of the coal at high temperatures.[12] Since quartz is primarily in its amorphous state and Al_2O_3 has ionic crystal structures with a high melting point, the ash fusion temperature (AFT) typically falls as the Si/Al ratio rises. Liu et al.[5] used synthetic ashes made of SiO_2, Al_2O_3, CaO, Fe_2O_3, and K_2O to study the relationships between coal

Received: June 10, 2023
Accepted: September 20, 2023
Published: October 11, 2023

ash compositions and AFTs. They discovered that the Si/Al ratio and Fe_2O_3 content increased with increasing ash content, and that K_2O had no discernible effect on the AFT. Meanwhile, the CaO effect had a minimum value for the AFT. When Chakravarty et al.[8] investigated the ash fusion behavior of Indian coals, they came to the same results that the presence of quartz led to the high AFT while the presence of Fe_2O_3 decreased the AFTs.[8] However, Song et al.[13] came to a different conclusion when they used coal mixtures in China with different additives. Their findings revealed that the effects of CaO, Fe_2O_3, and MgO displayed minimum values, whereas the AFTs always increased with increasing Si/Al ratios as a result of the formation of high melting point mullite and corundum. The fact that the different components always interact with one another, producing refractory minerals such as quartz, mullite, rutile, and kaolinite,[9] and low melting eutectics, suggests that the impact of ash composition on its fusion behavior is fairly complicated.

The characteristic that controls the behavior of ash in many coal-utilizing processes is termed AFT. Four characteristic temperatures are used to quantitatively characterize the melting characteristics and slagging performance of coal ash: softening temperature (ST), deformation temperature (DT), hemispherical temperature (HT), and flow temperature (FT).[14] The DT, is the temperature at which the coal ash starts to melt, leading to a high viscosity. At the ST, the viscosity of coal ash increases and the surface of the equipment becomes sticky. When the temperature reaches FT, the adhesion phenomena are already intense, and there is a significant volume of liquid phase present. The term "HT" is rarely used to describe the slagging process. Despite many studies on the relationship between coal ash components and AFT,[13,15−17] there is no universally known approach to predicting the AFT, and thus it is necessary to identify an appropriate method through research. The following are the characteristics and applications of these AFTs.

a. The understanding of the AFTs is commonly used by furnace and boiler operators and engineers in power plants to forecast the melting and sticking characteristics of coal ash.[18]
b. Provide crucial information on the amount to which ash agglomeration and clinkering are expected to occur in the combustor/gasifier.[19,20]
c. They represent the temperature range in which deposits on heat-absorbing surfaces could occur.[21]
d. They play a critical role in the operation of all types of gasifiers.[22] To allow continuous slug tapping, for example, the operating temperature in the entrained flow gasifiers must be higher than the FT.[23] AFTs determine the upper limit for the operating temperature at which ash agglomeration begins in fluid-bed gasifiers.[13]

Many studies have been conducted to predict the melting characteristic temperature of coal ash. Tambe et al.[24] used a computational intelligence model to estimate the coal ash melting temperature and obtained good results. Using the GWOSVM model, Xiao et al.[25] predicted the DT of coal ash and indicated that the model has a specific prediction accuracy. Tillman and Duong[26] examined the problem of slagging at Michigan's Monroe Power Plant. They used an online analyzer to examine the properties of the raw and blended coal in the study. The results of the online analyzer program were transformed into various characteristics such as the fuel volatility ratio, slagging alkalinity, etc. According to Tillman and Duong,[26] one of the most critical parameters in terms of slagging and

Table 1. Statistics of the Datasets Used for the Models[a]

	SiO_2	Al_2O_3	Fe_2O_3	P_2O_5	TiO_2	CaO	MgO	K_2O	Na_2O	SO_3	Ash	VM	FC	ST	HT	FT	DT
mean	50.78	30.02	4.66	0.98	1.65	5.77	1.42	0.796	0.37	2.82	16.98	25.56	62.64	1437.96	1453.98	1465.102	1418.673
SE	0.64	0.45	0.31	0.08	0.03	0.34	0.08	0.052	0.04	0.16	0.66	0.70	5.24	12.53	11.81	11.383	13.470
median	49.75	30.6	3.51	0.72	1.63	5.83	1.36	0.595	0.2	2.69	15.2	26.2	57.6	1420	1455	1470	1395
mode	47.4	33.9	2.82	0.17	1.55	8.13	1.85	0.46	0.12	4.31	13.1	26.9	60.5	1600	1600	1600	1600
std	6.329	4.488	3.05	0.77	0.34	3.41	0.76	0.514	0.44	1.58	6.57	6.91	51.89	124.08	116.94	112.68	133.34
kurtosis	0.259	−0.373	5.27	2.28	−0.23	0.22	−0.62	3.648	11.06	0.39	1.43	1.89	93.26	−1.534	−1.56	−1.55	−1.49
skewness	0.579	−0.221	1.81	1.32	0.35	0.36	0.26	1.937	2.911	0.40	1.29	−1.29	9.55	0.073	0.006	−0.041	0.135
range	34.4	22.4	18.94	4.11	1.49	15.95	3.2	2.7	2.79	8.04	33	31.5	526.4	370	350	340	400
minimum	36.9	17.5	0.76	0.15	1.06	0.15	0.04	0.22	0.05	0.02	7.1	5.6	38.6	1230	1250	1260	1200
maximum	71.3	39.9	19.7	4.26	2.55	16.1	3.24	2.92	2.84	8.06	40.1	37.1	565	1600	1600	1600	1600
count	98	98	98	98	98	98	98	98	98	97	98	98	98	98	98	98	98

[a]SE: standard error; Std: standard deviation; FC: Fixed carbon; VM: Volatile matter; Ash: Ash content.

https://doi.org/10.1021/acsomega.3c04113
ACS Omega 2023, 8, 39080−39095

Table 2. Simulated ANN Models for ST[a]

	AC-Ash-FC				AC-Ash-VM			
number of Neu	training	testing	validation	overall	training	testing	validation	overall
12−2−1	0.92518	0.76474	0.87412	0.89483	0.92281	0.76023	0.78992	0.87819
12−3−1	0.90967	0.9144	0.98671	0.92458	0.95517	0.97949	0.89712	0.94613
12−4−1	0.95075	0.98183	0.97493	0.95907	0.96716	0.95588	0.98597	0.9678
12−5−1	0.98576	0.98965	0.99455	0.9875	0.9736	0.99471	0.99707	0.98026
12−6−1	0.98148	0.99154	0.99323	0.9851	0.99449	0.97913	0.9978	0.99221
12−7−1	0.99003	0.99756	0.96695	0.98696	0.99604	0.99752	0.99769	0.99639
12−8−1	0.99455	0.99519	0.97509	0.9924	0.99719	0.99888	0.99398	0.99712
12−9−1	0.99272	0.98997	0.9935	0.99197	0.99745	0.98996	0.98423	0.99403
12−10−1	0.98909	0.9978	0.99477	0.9914	0.99718	0.99935	0.99924	0.99783
12−11−1	0.99235	0.98981	0.99126	0.99224	0.99856	0.99947	0.99986	0.99887
12−12−1	0.99892	0.97985	0.99478	0.99652	**0.99944**	**0.99976**	**0.99759**	**0.99922**
12−13−1	**0.99909**	**0.99884**	**0.99987**	**0.99918**	0.98233	0.99854	0.99594	0.98684
12−14−1	0.99331	0.98801	0.83433	0.96898	0.98635	0.99178	0.99188	0.98794
12−15−1	0.99727	0.99138	0.99974	0.99625	0.9941	0.99615	0.99984	0.99498
	AC-Ash-FC-VM							
13−2−1		0.91243		0.84385		0.92333		0.9045
13−3−1		0.90159		0.96978		0.96037		0.92093
13−4−1		0.97481		0.96893		0.98739		0.97407
13−5−1		0.97748		0.98783		0.97995		0.97906
13−6−1		0.98765		0.98166		0.99924		0.98847
13−7−1		0.97593		0.9927		0.99512		0.98188
13−8−1		0.98756		0.99649		0.98725		0.9887
13−9−1		**0.9953**		**0.99748**		**0.99947**		**0.99621**
13−10−1		0.98848		0.98988		0.96802		0.9848
13−11−1		0.99291		0.99356		0.99657		0.99348
13−12−1		0.99268		0.99968		0.99391		0.99402
13−13−1		0.9893		0.99883		0.99724		0.99202
13−14−1		0.99132		0.99978		0.98652		0.99169
13−15−1		0.97585		0.97632		0.97695		0.97758

[a]Bolded values indicate the parameters with the highest coefficients of correlation (R).

fouling potential is the VM level of the fuel (coal or blend). Also, according to the study investigated on biomass samples by Holubcik et al.,[27] ash melting temperatures change in accordance with the chemical composition of ash. Similarly, the majority of past research shows that AFTs are linked to the chemical composition of coal ash samples.[5] According to Bilen and Kizgut,[28] the VM content of coal plays a significant role in slagging and fouling potential. To estimate coal ash DT, Wang et al.[29] used the traditional linear regression, Factsage calculation, and back-propagation (BP) neural network calculation. The linear regression predicts the change trend of coal ash DT; however, the results are not very good. The Factsage's calculations reveal a significant difference from the experimental values, while the BP neural network's prediction results were accurate, with a maximum relative average error of 6.67%.

Through a number of studies, Yu et al.[6] indicates the relationship between coal ash chemical composition and ST, and developed a more precise ST prediction method. Based on the studies mentioned above, we can see that a number of research approaches to estimate the temperature of the melting characteristics of coal ash have been proposed. Empirical formulas, software prediction, and mathematical modeling are the most common methods used. Because AFT information is important in the design, operation, and optimization of coal combustion liquefaction and gasification processes, a range of mathematical models for their prediction have been created. Models with improved prediction accuracy and broader applicability are still being developed. The majority of the previous models were created with data from coal samples from a few geographic areas or from a single location. AFT coal models from one or a few geographical regions have limited applicability, because coal from different regions may have different chemical and physical characteristics. Some existing AFT prediction models take into account coal from multiple geographic regions, while these models also have a relatively high precision of prediction.[18,19] However, because they are dependent on a high number of predictors (input variables), the models are complex, expensive, and time-consuming for experimentation. This reduces their generalization ability and the time needed to compile predictor data. Hence, this study aimed to develop AFT predictive models for coal samples from South African coalfields based on their proximate analysis using a soft computing tool. It is also aimed at investigating the feasibility of using ANNs to predict the AFTs, taking into consideration the effect of proximate analysis data.

The way coal burns, the amount of heat it produces, and the amount of ash left behind are used to determine its quality. The amount of carbon, hydrogen, and noncombustible materials in the coal determines these properties.[8] There are two distinct approaches used to analyze coal's properties: ultimate and proximal analysis. The ultimate analysis, which normally takes place in a laboratory, is highly expensive and determines the precise elemental composition of the coal. In contrast to the proximate analysis, which is very simple to conduct and calls for only common equipment and analysts with moderate training,

https://doi.org/10.1021/acsomega.3c04113
ACS Omega 2023, 8, 39080−39095

Table 3. Simulated ANN Models for HT[a]

	AC-Ash-FC				AC-Ash-VM			
no of neurons	training	testing	validation	overall	training	testing	validation	overall
12−2−1	0.91437	0.9526	0.84029	0.91146	0.92014	0.82591	0.84571	0.89463
12−3−1	0.96373	0.93082	0.95919	0.95578	0.97112	0.94499	0.98806	0.96788
12−4−1	0.96887	0.97837	0.98352	0.97087	0.98402	0.93219	0.97813	0.97412
12−5−1	0.98954	0.87691	0.98522	0.96601	0.9899	0.99056	0.99791	0.99085
12−6−1	0.99355	0.99878	0.99812	0.99525	0.98766	0.99336	0.99697	0.98993
12−7−1	0.99172	0.95954	0.96938	0.98306	0.99275	0.99902	0.99842	0.99446
12−8−1	0.99538	0.99526	0.99616	0.99558	0.98844	0.99709	0.96535	0.98714
12−9−1	0.99298	0.98684	0.99491	0.99219	0.97637	0.9994	0.98322	0.98051
12−10−1	0.99488	0.98678	0.99861	0.99428	**0.99858**	**0.99987**	**0.99991**	**0.99898**
12−11−1	0.99517	0.9906	0.99844	0.99497	0.99936	0.98478	0.99796	0.99699
12−12−1	**0.99867**	**0.99813**	**0.99923**	**0.99867**	0.99174	0.99998	0.99981	0.99377
12−13−1	0.99101	0.99794	0.99538	0.99274	0.98689	1	0.99772	0.9902
12−14−1	0.9991	0.9956	0.99923	0.99842	0.99739	0.99993	0.99984	0.99816
12−15−1	1	0.98101	0.99184	0.99533	0.99465	0.99785	0.99781	0.99535
	AC-Ash-FC-VM							
13−2−1		0.92676		0.82529		0.91023		0.90822
13−3−1		0.96407		0.98779		0.96645		0.96826
13−4−1		0.95694		0.95363		0.98842		0.96204
13−5−1		0.97571		0.96002		0.99122		0.97428
13−6−1		0.9874		0.97666		0.9931		0.98575
13−7−1		0.9976		0.98741		0.99858		0.99641
13−8−1		0.99892		0.99856		0.98916		0.99599
13−9−1		**0.99881**		**0.99934**		**0.99745**		**0.99876**
13−10−1		0.99894		0.99903		0.98887		0.9972
13−11−1		0.985		0.99753		0.99725		0.98885
13−12−1		0.9914		0.99971		0.98459		0.99181
13−13−1		0.99779		0.9867		0.99936		0.99627
13−14−1		0.99948		0.99381		0.99915		0.99841
13−15−1		0.99946		0.98271		0.99972		0.99804

[a]Bolded values indicate the parameters with the highest coefficients of correlation (R).

the ultimate analysis and petrographic composition of coal require the use of sophisticated equipment and expertise.

A variety of extremely complicated and nonlinear phenomena can be modeled and studied using artificial neural networks (ANN), which are effective modeling and investigation methods. While having a pretty good level of prediction accuracy, some current AFT prediction models consider coal from various geographic regions.[24] The models are complicated, costly, and time-consuming to test since they depend on a large number of predictors (input variables). As a result, they are less able to generalize, and it takes longer to gather predictor data. The AFTs have been predicted by using a variety of correlations. Prediction of the AFTs from ultimate analysis and ash chemistry is the most commonly utilized method.[5] Because of this correlation, the predictions have varying average absolute and bias errors.[7] The majority of these generalized correlations, however, suffer from the issue of requiring ultimate analysis and ash chemistry data as input data, which necessitates expensive tools and highly qualified analysts. However, there has been no research that examines the outcomes of soft computing tools to explain how proximate analysis data affects AFTs. The present study describes the development and training of a multiple input, single output ANN (MISO-ANN), which is used to predict AFTs from ash chemistry and proximate analysis data. The ultimate objective is to enhance the performance of the combustion control system with the aid of knowledge of the proximate content of coal. In addition, the present study aims to demonstrate that ANNs are capable of accurately predicting AFTs in coal from proximate analysis and ash chemistry. The outcome of this prediction will evaluate the effect of proximate parameters with the most suitable predictive model.

2. MATERIALS AND METHODS

2.1. Experimental Method. A total of 98 coal samples were collected from different South African coalfields for this study. Samples were taken from various mines on the Witbank coal field, covering Middleburg and Secunda, as well as the Ermelo coal field (Belfast − Carolina) and the Kangwane coal field. Some samples were also collected from the Northern province/Limpopo (Venda and Ellisras), the Free State, and the Vereeniging coal fields (Sasolburg). In addition, samples were also taken from coalfields of Vryheid, Utrecht, and Ulundi, in the native Kwazulu Natal. These samples from the individual coal fields were all formed during the Permian Period to the mid-Triassic Period and are in the Gondwana Karoo Basin. These coals are less mature and have different properties (mineral matter and organic composition) than carboniferous coal in the northern hemisphere.

The samples were pulverized to a −212 μm size fraction, blended, and divided using a rotary splitter to generate different subsamples in accordance with ref 30, prior to ashing. Inductively coupled plasma optical emission spectrometry (ICP-OES) was used to conduct a compositional analysis of the ash in coal samples in accordance with ref 30, to identify the oxides of the major elements for the coal ash (ashed to 815 °C),

https://doi.org/10.1021/acsomega.3c04113
ACS Omega 2023, 8, 39080−39095

Table 4. Simulated ANN Models for FC[a]

	FT-Ash-FC				FT-Ash-VM			
no of neurons	training	testing	validation	overall	training	testing	validation	overall
12−2−1	0.8771	0.81812	0.83769	0.86317	0.95524	0.87082	0.88253	0.9305
12−3−1	0.97291	0.91877	0.99587	0.96749	0.97052	0.85595	0.91775	0.94493
12−4−1	0.96922	0.8873	0.98668	0.95523	0.97614	0.98836	0.98262	0.97841
12−5−1	0.98384	0.91738	0.9662	0.96993	0.98587	0.98965	0.99049	0.98723
12−6−1	0.98474	0.99893	0.99361	0.98872	0.99144	0.99337	0.99597	0.9926
12−7−1	0.99461	0.98559	0.98593	0.99159	0.99351	0.99815	0.99705	0.99434
12−8−1'	0.99209	0.99871	0.99298	0.99336	0.99515	0.99951	0.97929	0.99436
12−9−1	0.99014	0.99861	0.998	0.99257	0.98738	0.98869	0.98394	0.98686
12−10−1	0.98927	0.99723	0.99983	0.99231	0.99335	0.99636	0.99842	0.99461
12−11−1	**0.99992**	**0.99997**	**0.99491**	**0.99948**	0.99984	0.98316	0.99986	0.99693
12−12−1	0.98725	0.98441	9.99704	0.9878	**0.99972**	**0.99887**	**0.99958**	**0.99962**
12−13−1	0.99221	0.99766	0.99578	0.99336	0.99517	0.99975	0.99996	0.99653
12−14−1	0.99983	0.98528	0.99651	0.99679	0.99943	0.99844	0.9995	0.99925
12−15−1	0.99128	0.99433	0.999	0.99265	0.99326	0.99925	0.99791	0.9948
	FT-Ash-FC-VM							
13−2−1		0.89992		0.90546		0.91476		0.90041
13−3−1		0.95531		0.98542		0.85716		0.94229
13−4−1		0.95883		0.98236		0.98939		0.967
13−5−1		0.9892		0.98517		0.9629		0.98361
13−6−1		0.99417		0.99582		0.9997		0.99508
13−7−1		0.99581		0.99795		0.99665		0.99639
13−8−1		0.99317		0.99033		0.9677		0.98858
13−9−1		0.98512		0.98888		0.9789		0.98551
13−10−1		**0.99847**		**0.99883**		**0.99993**		**0.99873**
13−11−1		0.98922		0.99363		0.99565		0.99057
13−12−1		0.99702		0.99939		0.99671		0.99744
13−13−1		0.99402		0.99728		0.98638		0.99345
13−14−1		0.99261		0.99658		0.99737		0.99393
13−15−1		0.99827		0.9981		0.99934		0.9985

[a]Bolded values indicate the parameters with the highest coefficients of correlation (R).

including SiO_2, Al_2O_3, CaO, K_2O, Na_2O, Fe_2O_3, MgO, TiO_2, P_2O_5, and SO_3. The coal ash samples were prepared using lithium tetraborate fusion in a platinum crucible, and they were then leached in diluted hydrochloric acid to bring them into solution. To ascertain the proportion of all oxides in the ash, the solutions were examined by ICP-OES. The characteristic fusion temperatures of the ash were based on the standard ash fusion test, ISO 540. The coal sample was first ashed in a thin layer at 815 °C to give an adequate amount of ash for the test. The formed ashes were prepared as pyramids according to ISO 540. The samples were heated in CO_2-atmosphere at a heating rate of 10 K/min from 700 °C up to 1500 °C. The stages of fusion, such as initial DT, ST, HT, and FT, were recorded for interpretation. The proximate analysis was completed in accordance with the following guidelines[31]. The fixed carbon was expressed as the 100% minus (ash content + VM + moisture content). The statistics of the outcome of the experimental results are presented in Table 1, while the details of the adopted data set from the experimental outcomes are presented in Appendix (Tables A1−A3).

2.2. Prediction Method. Theoretical, statistical, empirical, and more recently, artificial intelligence (AI) and data-driven modeling methodologies have all been used in various studies on AFT prediction.[7] A number of optimization algorithms have been proposed and used to solve various optimization problems, including evolutionary-based, population-based incremental learning (PBIL), biogeography-based optimizer (BBO), simulation annealing (SA), black hole optimization algorithm, galaxy-based optimization algorithm, particle swarm optimization (PSO), ant colony optimization (ACO), and artificial bee colony (ABC).[7] Some of the aforementioned algorithms show excellent results in locating a worldwide optimal solution. According to the "no free lunch" principle, none of these algorithms, however, can ensure the best answer for every situation; therefore, many more methods can be tested. In terms of explorative strength, ANN have been used to deliver consistent performance to solve complicated nonlinear physical world issues.

The ANN, a machine learning (ML) model that has been adopted in this study, has demonstrated significantly better predictive accuracy than those of many other emerging ML models. For instance, Bui et al.[32] used k-nearest neighbors, ANN, random forest, support vector regression, Gaussian process, Bayesian additive regression trees, and boosted regression trees to forecast the blast-induced air overpressure. In their research, ANN performed better than the other models. For the purpose of predicting ground settlement, Tang and Na[33] also evaluated the efficacies of a variety of ML techniques, including support vector machines (SVM), random forests (RF), back-propagation neural networks (BPNN), and deep neural networks (DNN).

An empirical modeling tool that mimics the behavior of biological brain structures is called the ANN. Using simply the input-output data, neural networks are a potent tool that can reveal underlying, very complicated relationships.[34] ANNs, and in particular feed-forward ANNs (FANNs), have been widely

https://doi.org/10.1021/acsomega.3c04113
ACS Omega 2023, 8, 39080−39095

Table 5. Simulated ANN Models for DT[a]

	DT-Ash-FC				DT-Ash-VM			
no of neurons	training	testing	validation	overall	training	testing	validation	overall
12−2−1	0.94191	0.97639	0.75077	0.91943	0.93742	0.82326	0.81978	0.90343
12−3−1	0.92213	0.98372	0.92446	0.93063	0.96787	0.97734	0.97094	0.96939
12−4−1	0.94675	0.98526	0.95548	0.95382	0.93183	0.95682	0.79481	0.91863
12−5−1	0.98346	0.96	0.98833	0.97889	0.97722	0.96886	0.98656	0.97386
12−6−1	0.98922	0.98178	0.99898	0.98969	0.98566	0.99204	0.99827	0.98865
12−7−1	0.996	0.99418	0.98788	0.99449	0.99107	0.99014	0.99598	0.99162
12−8−1	0.99257	0.99738	0.9421	0.98812	0.98853	0.91017	0.96155	0.96913
12−9−1	0.99674	0.99708	0.9989	0.99692	0.98548	0.97892	0.99172	0.98519
12−10−1	0.99469	0.99797	0.99751	0.99564	**0.99694**	**0.9997**	**0.99761**	**0.99745**
12−11−1	0.99864	0.99255	0.99888	0.99783	0.99486	0.99888	0.99587	0.99574
12−12−1	0.99894	0.99118	0.9983	0.99797	0.99251	0.99992	0.99999	0.99409
12−13−1	0.99195	0.99501	0.99411	0.99279	0.99391	0.99711	0.99995	0.99545
12−14−1	0.96349	0.9734	0.98724	0.96904	0.96183	0.99823	0.99845	0.97289
12−15−1	**0.99846**	**0.99915**	**0.99893**	**0.99862**	0.99586	0.99801	0.9994	0.9966
	DT-Ash-FC-VM							
13−2−1	0.9158	0.86776	0.90656	0.9098				
13−3−1	0.94482	0.92309	0.9514	0.94301				
13−4−1	0.98404	0.98001	0.98252	0.9827				
13−5−1	0.98437	0.98007	0.9818	0.98347				
13−6−1	0.99229	0.99608	0.99042	0.99234				
13−7−1	0.98576	0.99459	0.98924	0.98816				
13−8−1	0.98405	0.99787	0.97544	0.9851				
13−9−1	0.98011	0.98521	0.98674	0.98156				
13−10−1	0.99218	0.99857	0.99772	0.99397				
13−11−1	0.98429	0.95551	0.99128	0.9811				
13−12−1	**0.99823**	**0.99965**	**0.99987**	**0.99866**				
13−13−1	0.97672	0.98344	0.97894	0.97774				
13−14−1	0.97845	0.99702	0.98581	0.98215				
13−15−1	0.95197	0.99327	0.98935	0.96716				

[a]Bolded values indicate the parameters with the highest coefficients of correlation (R).

explored over the past ten years to present process models, and their use in industry has been expanding quickly.[7] The fundamental benefit of ANN is its capability to model a problem using examples rather than an analytical description (i.e., data-driven). Additionally, ANNs are particularly adept at effectively representing complicated nonlinear systems. As a nonlinear statistical identification method, it is also regarded as such.[35] The architecture (number of layers), topology (connective pattern, feed-forward or recurrent, etc.), and learning regime of neural networks are used to classify them. Error BP learning and multilayered feed-forward networks are used in the majority of power system applications.[36] The current study uses an MISO-ANN, which is the most widely used generalized neural network at the moment and is also the easiest to develop. The approach of proximate analysis data used in this study to predict the AFTs has not been reported by researchers, and the outputs from these models have shown promising and reliable predictive abilities.

To develop predictive models for the prediction of the AFTs, the most used AI method is the ANN. The ANN imitates the interconnectivity and functionality of the neurons in the human brain to perform its functions. The ANN learns from a given example and applies the residual knowledge to future prediction. This tool has been used in solving various complex engineering problems as indicated by Lawal and Kwon,[34] Onifade et al.,[35] Abdulsalam et al.,[37] Akinwekomi and Lawal,[38] etc.

To perform the ANN model in this study, the MISO-ANN model is developed for the prediction of the AFTs. For each of the AFTs, three models are proposed, making 9 models in total. The ten primary oxides present in coal ashes (SiO_2, Al_2O_3, Fe_2O_3, P_2O_5, TiO_2, CaO, MgO, K_2O, Na_2O, and SO_3) tagged AC in this study are used in conjunction with the ash content and the fixed carbon, ash content and VM, ash content, fixed carbon and VM. There are 12 inputs in 6 of the models, while there are 13 inputs in three of the remaining models. The ST, HT, FT, and DT are the targeted outputs in three models out of the 12 (12) models. The ANN models are implemented in the MATLAB software by importing the model parameters and normalizing the data in line with the selected kernel parameters. The three-layer ANN structures are considered for all the models with the BP training algorithms. The transfer function used in the hidden and output layers is hyperbolic tangent, while the training function adopted is Leveberg-Marquardt. The number of neurons is varied between 2 and 15. The optimum trained network for the models is selected based on the models' output during the variation of the hidden layer neurons. This is presented in detail in the Results and Discussion section.

3. RESULTS AND DISCUSSION

The coal samples were characterized in terms of their ash content, VM, and fixed carbon, while the coal ash samples were characterized in terms of their AFTs as ST, HT, FT, and DT. A database of the AFTs, proximate analysis, and ash chemistry analyses data obtained from the experimental tests for the coal samples are presented in Tables A1−A3 of Appendix. The obtained experimental results are modeled using ANN to

https://doi.org/10.1021/acsomega.3c04113
ACS Omega 2023, 8, 39080−39095

Table 6. Relative Errors for Testing and Validation Phases

models	testing				validation			
	relative error (RE) in the predicted							
	ST	HT	FT	DT	ST	HT	FT	DT
AC-Ash-FC	−0.28149	0.102053	−0.0075	−0.01613	0.02951	−0.0056507	0.042886	−0.0195
	0.226658	−0.01264	−0.0241	−0.06777	0.070808	0.0630031	0.027209	−0.57723
	0.04104	0.024426	0.005844	0.006162	0.069153	0.087943	0.00047	0.041136
	0.035452	−0.00155	−0.00298	1.042542	0.203488	−0.0036185	0.021681	0.241088
	−0.03391	1.382204	0.109344	0.053185	0.020593	−0.837841	0.003638	0.059358
	0.056419	0.023839	−0.00543	−0.00755	0.021994	0.0014146	0.002248	0.13489
	−0.01387	0.008018	0.029417	−0.01196	0.001419	0.2599479	−0.01207	−0.06198
	−1.12826	0.027657	0.011115	−0.54235	0.245957	0.1231976	−0.00229	0.000831
	0.036518	−0.53781	2.65×10^{-06}	−0.58693	0.102192	−0.0024453	0.002198	−0.03577
	−0.01572	−0.00756	0.009168	0.230934	1.96×10^{-08}	−0.4978605	2.470341	0.066342
	0.077845	−0.02651	0.001316	0.000712	0.056244	0.0619302	−0.00419	1.409313
	−0.88515	0.159824	0.056512	−0.00139	0.037549	−0.2649845	0.006225	−0.25733
	−0.02519	0.15451	−0.02239	−0.02173	−0.35979	−0.0103312	0.003579	−0.04141
	0.020889	0.027138	0.210934	−0.92545	0.03063	0.4115554	−0.00256	−0.00582
	0.011696	0.001025	−0.0574	−0.02282	0.320156	0.0273792	0.000213	0.165422
MARE	0.192674	0.16645	0.036896	0.235841	0.104632	0.1772735	0.173453	0.207828
AC-Ash-VM	−0.04799	0.093563	−0.04594	0.523886	0.009256	0.0200703	0.001667	0.021936
	−0.02612	0.016625	0.067303	0.059845	0.212884	0.0568296	−0.0102	0.138322
	0.010041	−0.2153	0.096819	−0.13508	0.001014	−0.158811	0.001221	−0.04646
	0.052152	−0.18111	0.015933	0.054816	1.897386	0.1157396	−0.22822	0.35826
	0.13204	0.039445	0.420035	0.038646	−0.01081	0.0022122	0.017551	0.003674
	−0.04356	−0.12027	−0.02708	−0.63049	0.002506	0.0034216	−0.02143	−2.51634
	−0.00345	−0.11529	−0.24164	−0.00806	0.244318	0.3096374	0.284188	0.154804
	−0.00187	−0.18462	−0.00534	−0.20668	0.768103	−0.1315117	−0.02692	0.166486
	−0.04566	−0.02761	−0.01688	0.204574	0.105958	0.0290103	0.115546	−0.00837
	0.430306	0.029081	−0.48027	−0.89118	0.00985	0.0082795	−0.01297	0.20143
	0.433044	0.063491	−0.30955	0.230462	0.002131	0.0475901	0.044425	0.175829
	−0.03913	−0.0069	−0.01285	0.057396	−0.05542	−0.057492	0.032011	0.006156
	0.011502	−0.41034	−0.64537	−0.02717	−0.03213	−0.0357868	−0.54651	−0.05961
	0.021776	0.011482	0.554659	0.005999	−0.92115	0.0312063	0.452012	−0.01382
	0.045754	−0.23831	0.022261	0.040096	−0.01378	0.2805559	0.021822	0.005623
MARE	0.089625	0.116897	0.197462	0.207625	0.28578	0.085877	0.121114	0.258475
AC-Ash-FC-VM	−0.04656	−0.86268	−0.04516	0.083089	0.151174	0.8656918	−0.00978	−0.14831
	0.054857	3.29×10^{-05}	−0.001	0.004321	0.085844	0.0407569	0.063054	0.194006
	−0.03049	−0.0614	1.130509	−0.00661	−0.12203	0.0438664	3.49×10^{-05}	0.015899
	−0.11202	−0.1116	0.186245	0.056244	−0.2716	−0.1601615	0.286303	0.056112
	0.005329	−0.03415	0.095947	0.001312	-1.8×10^{-07}	−0.0087387	−0.07516	−0.00475
	0.057009	−0.00161	−0.59826	0.913098	−0.66684	0.1377956	0.00789	0.011926
	−0.04094	0.005866	−0.13026	0.058761	0.085833	−0.0012979	−0.03718	−0.02709
	−0.59758	−0.18407	1.41×10^{-05}	−0.04108	−0.25004	−0.2849889	−0.02517	−0.34904
	0.29496	0.648591	0.020097	−0.05592	0.459316	0.1164743	−0.01108	0.068225
	0.04044	0.024108	0.257414	0.14436	0.104564	−1.4215049	−0.03511	0.000309
	−0.00208	−0.05862	0.034095	−0.06795	0.098506	−0.1034133	0.079429	−0.03022
	0.06766	0.420255	−0.01921	−0.0324	−0.01525	−0.0017185	0.004677	−0.35394
	0.282316	−0.70093	−0.01539	0.042059	−0.02429	0.0288712	−0.07165	0.123852
	−2.61465	−0.01059	−0.32825	0.030063	0.100137	0.0141752	0.164283	−0.01228
	0.052353	0.033384	0.002233	0.035278	−0.05872	−0.908337	0.020801	−0.01582
MARE	0.286617	0.210525	0.190938	0.104837	0.166277	0.2758528	0.05944	0.09412

establish which combination of the proximate parameters will give the best ash chemistry. About 168 models were developed among which 12 models were selected, that is, three models for each of the AFTs for further analyses as presented below.

3.1. Variation of the Hidden Neurons for Optimum ANN Structure. The results obtained for the 168 simulated ANN networks are presented in Tables 2−5 for the ST, HT, FT, and DT, with varying proximate analysis parameters. With regard to ST, the 12−13−1 ANN structures outperformed the other models out of the 14 (14) ANN structures simulated. When the VM is used with AC and Ash excluding FC, the 12−12−1 ANN structures appear to be the optimum structure out of the 14 ANN structures tried. When FC is used with AC and Ash including VM, the 12−9−1 ANN structures appear to be the best with the highest performance indicator values. For the ST, the model with the VM, AC, and Ash excluding the FC, appears to be the best combination.

https://doi.org/10.1021/acsomega.3c04113
ACS Omega 2023, 8, 39080−39095

Table 7. TS Results

	TS values at 0.2%			
models	ST	HT	FT	DT
training				
AC-Ash-FC	73.33	86.67	93.33	66.67
AC-Ash-VM	86.67	80.00	60.00	73.33
AC-Ash-FC-VM	73.33	73.33	73.33	93.33
validation				
AC-Ash-FC	73.33	66.67	93.33	73.33
AC-Ash-VM	66.67	86.67	73.33	86.67
AC-Ash-FC-VM	73.33	80.00	93.33	86.67

For the HT, the same number of models with the same model parameters were also tried. The models obtained revealed that 12−12−1 is the best for the AC-Ash-FC, while 12−10−1 is the best for the AC-Ash-VM, and for the AC-Ash-FC-VM, 13−19−1 outperformed the others. With regard to FT, the best ANN structure for the AC-Ash-FC is 12−11−1, while that of AC-Ash-VM is 12−12−1 and that of AC-Ash-FC-VM is 13−10−1. For the DT, the best ANN structure for the AC-Ash-FC is 12−15−1, for the AC-Ash-VM is 12−10−1, while that of the AC-Ash-FC-VM is 13−12−1. A typical example of the selected ANN structures with the marginal plot is presented in Figure 1. The example shown is for the DT with regard to of AC-Ash-FC-VM.

3.2. Selection of the Best AFT Models Based on the Variation in Proximate Analysis Parameters. *3.2.1. Error Bars and Coefficient of Determination Approach.* The selection of the best AFT models based on AC and the variations in proximate analysis parameters is presented herein. The first approach adopted is to plot the training, testing, and validation data sets as obtained from the models for each temperatures ST, HT, FT, and DT as presented in Figures 2−5 within the error bars. For the ST (Figure 2), all the predicted data sets fall within ±3% error bars with regard to the AC-Ash-FC and AC-Ash-VM while at least one data point falls outside the −3% error bar with regard to AC-Ash-FC-VM. Based on this, the R-value obtained for the training in AC-Ash-FC-VM is the lowest. With regard to HT (Figure 3), all the data points fall within the error bars for the AC-Ash-FC, AC-Ash-VM, and AC-Ash-FC-VM. However, the data points for AC-Ash-VM largely fall very close to the fitted line, most specifically for the testing and validation. Based on the closeness of the data sets to the fitted line, the R-values of the AC-Ash-VM for the testing and validation are greater than other combinations of the proximate analyses parameters. With regard to FT (Figure 4), all the data

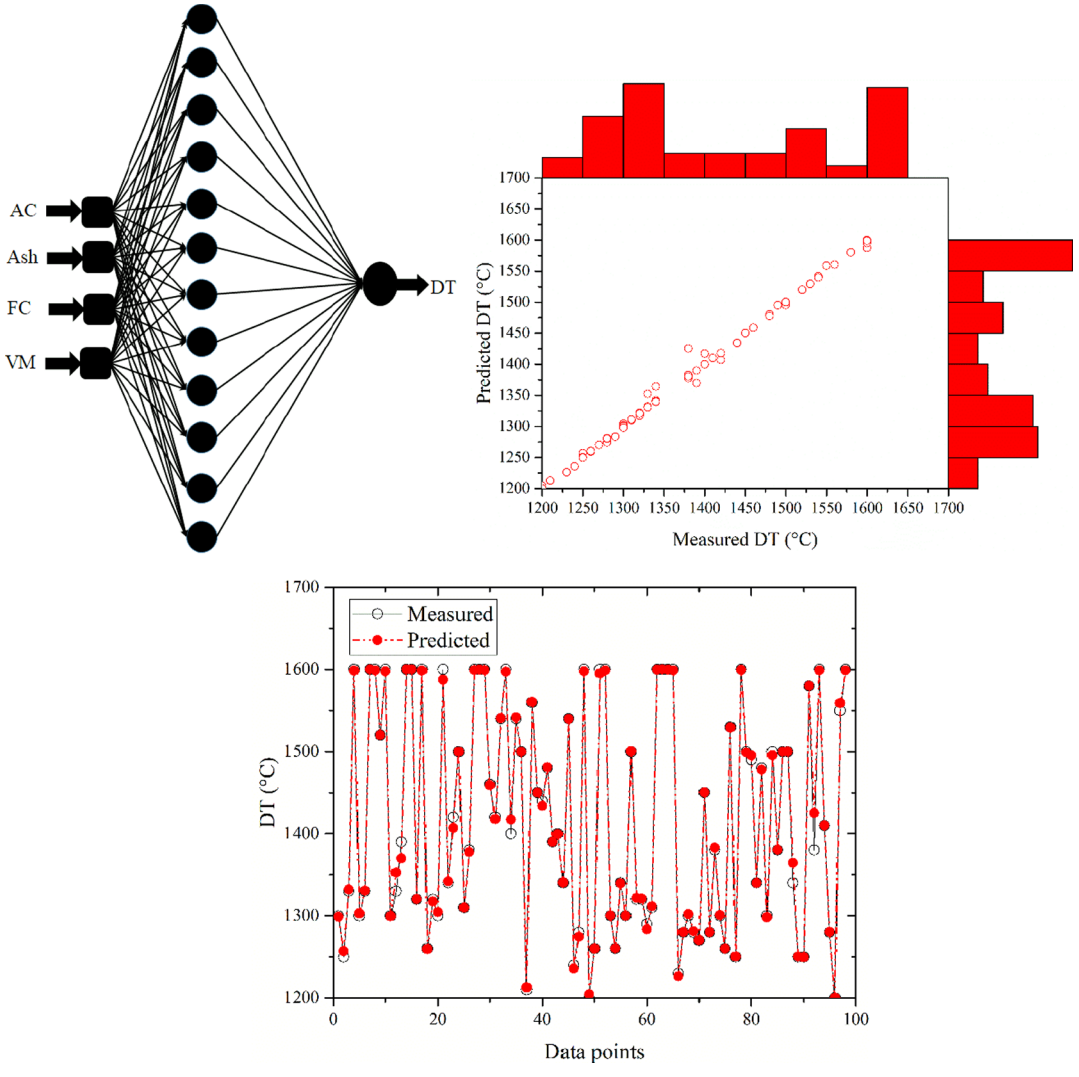

Figure 1. Typical example of the optimum ANN architecture.

https://doi.org/10.1021/acsomega.3c04113
ACS Omega 2023, 8, 39080−39095

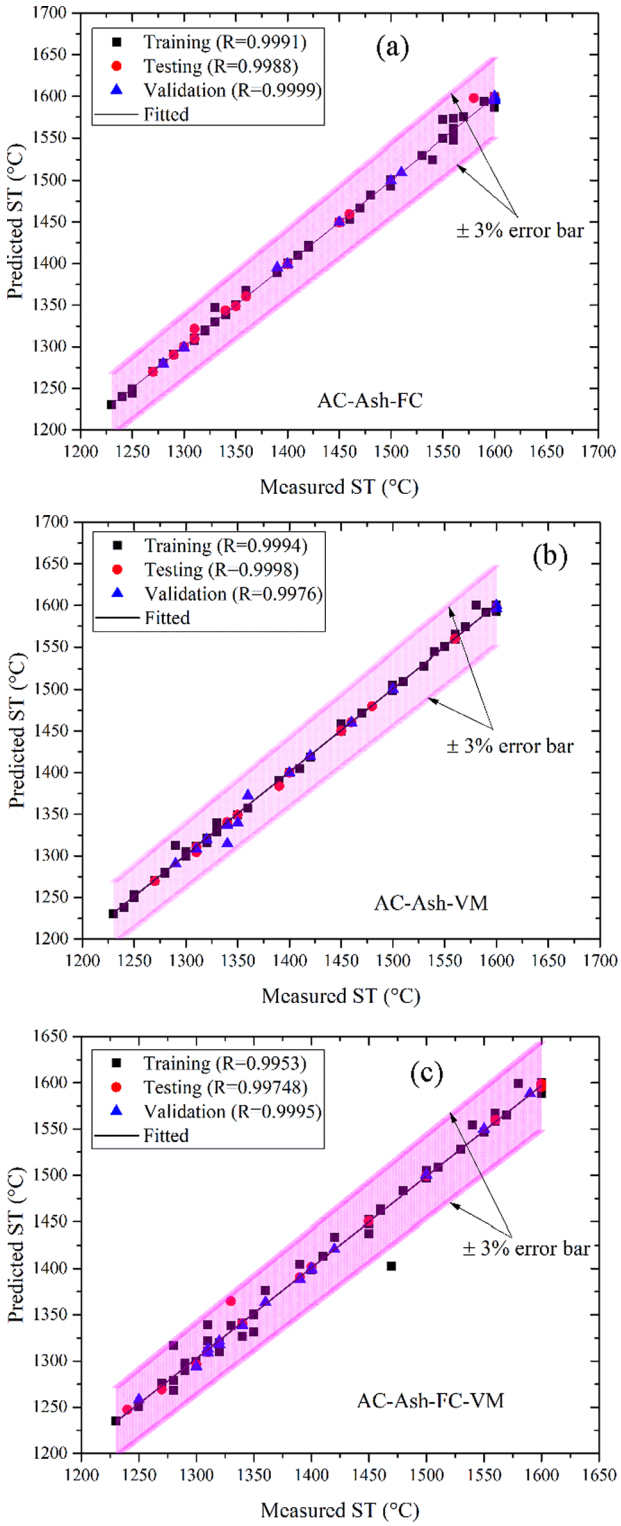

Figure 2. ST predicted using (a) AFT-Ash-FC, (b) AFT-Ash-VM, and (c) AFT-Ash-FC-VM.

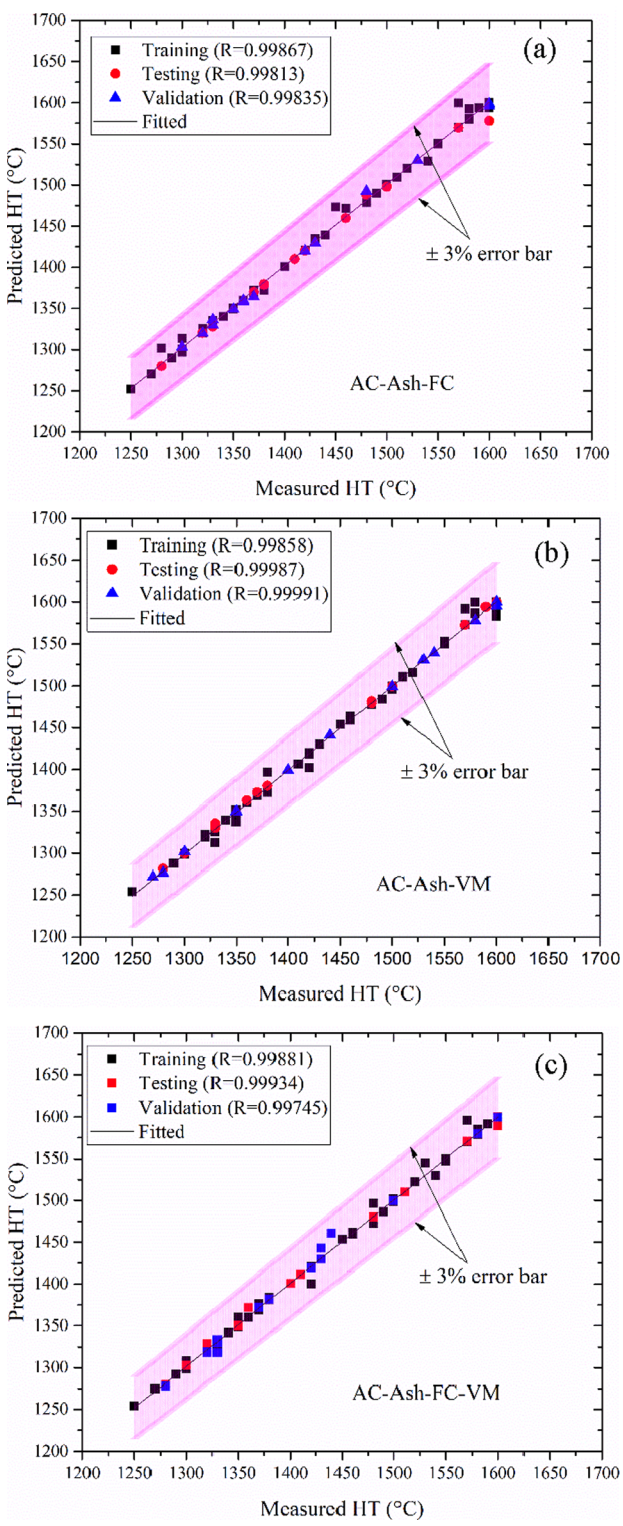

Figure 3. HT predicted using (a) AFT-Ash-FC, (b) AFT-Ash-VM, and (c) AFT-Ash-FC-VM.

points fall within the error bars for the AC-Ash-FC, AC-Ash-VM, and AC-Ash-FC-VM. However, a data point in the validation of AC-Ash-FT falls almost on the −3% error bar which gives rise to the low R-value obtained for the validation as compared with the training and testing. Some data points with regard to AC-Ash-FC-VM disperse from the fitted line. The R-values of the AC-Ash-VM seems to be evenly distributed around the fitted line. For the DT (Figure 5), the data points predicted for the AC-Ash-VM dispersed for the training, testing, and validation data sets compared to the AC-Ash-FC and AC-Ash-FC-VM. However, all the data fall within the error bars except one point each with regards to AC-Ash-FC and AC-Ash-FC-VM which are lying on the +3% error bars. With regard to ST, HT and FT, AC-Ash-VM seems to be better while for DT, AC-Ash-

https://doi.org/10.1021/acsomega.3c04113
ACS Omega 2023, 8, 39080−39095

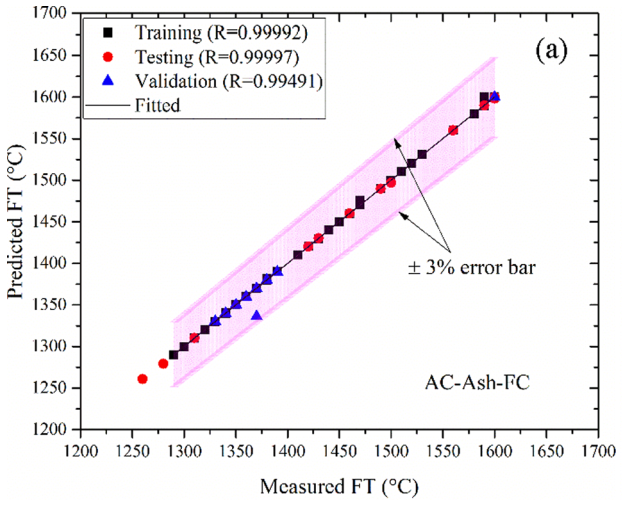

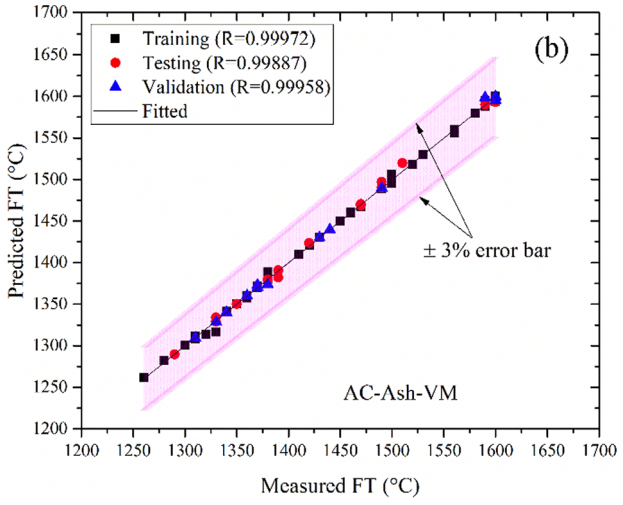

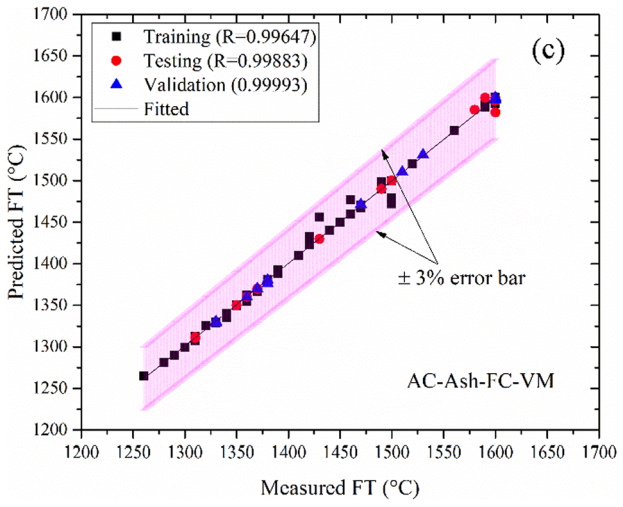

Figure 4. FT predicted using (a) AFT-Ash-FC, (b) AFT-Ash-VM, and (c) AFT-Ash-FC-VM.

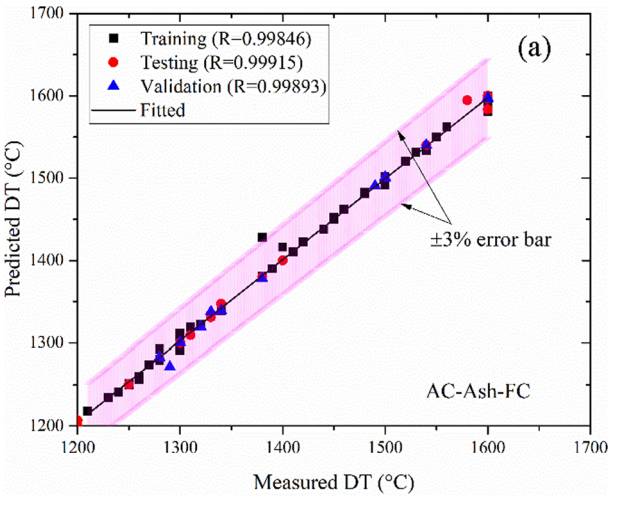

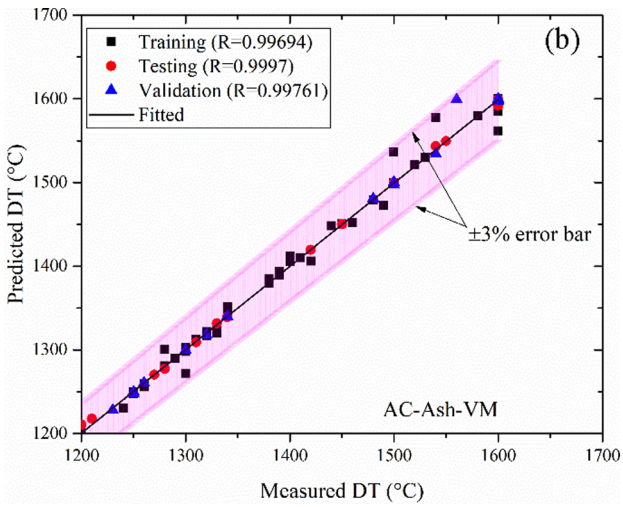

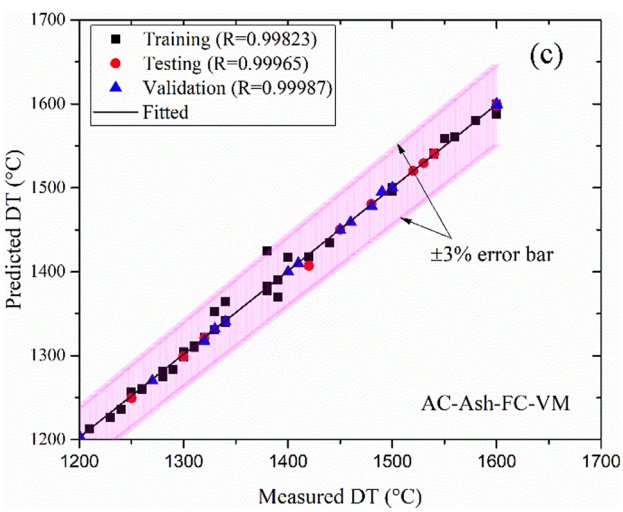

Figure 5. DT predicted using (a) AFT-Ash-FC, (b) AFT-Ash-VM, and (c) AFT-Ash-FC-VM.

FC-VM seems to be the best. However, this selection is not clear enough as the correlation coefficient is considered as a weak statistical indicator.[39] Therefore, a more rigorous statistical approach is employed to give a reliable selection of the best combination of parameters for the ST, HT, FT, and DT as presented in Figures 2−5.

3.2.2. Threshold Statistics Approach. The threshold statistic approach proposed by Jain et al.[40] is adopted in this study to establish which of the models based on the combination of the proximate analysis parameters is the best. To employ this method, the percentage relative error (RE) and the mean absolute percentage relative error (MARE) are first computed by using eqs 1 and 2.

https://doi.org/10.1021/acsomega.3c04113
ACS Omega 2023, 8, 39080−39095

Table A1. AFT Analyses

	AFT (°C)					AFT (°C)			
sample	DT	ST	HT	FT	sample	DT	ST	HT	FT
1	1300	1320	1330	1340	50	1260	1290	1300	1320
2	1250	1280	1300	1310	51	1600	1600	1600	1600
3	1330	1340	1350	1360	52	1600	1600	1600	1600
4	1600	1600	1600	1600	53	1300	1310	1320	1330
5	1300	1340	1380	1390	54	1260	1320	1350	1380
6	1330	1340	1350	1360	55	1340	1350	1360	1370
7	1600	1600	1600	1600	56	1300	1310	1320	1330
8	1600	1600	1600	1600	57	1500	1530	1550	1560
9	1520	1540	1550	1560	58	1320	1350	1370	1380
10	1600	1600	1600	1600	59	1320	1340	1350	1360
11	1300	1310	1320	1330	60	1290	1310	1330	1350
12	1330	1340	1360	1370	61	1310	1320	1330	1340
13	1390	1450	1460	1470	62	1600	1600	1600	1600
14	1600	1600	1600	1600	63	1600	1600	1600	1600
15	1600	1600	1600	1600	64	1600	1600	1600	1600
16	1320	1390	1400	1410	65	1600	1600	1600	1600
17	1600	1600	1600	1600	66	1230	1250	1270	1280
18	1260	1280	1300	1310	67	1280	1300	1360	1370
19	1320	1350	1370	1380	68	1300	1330	1350	1370
20	1300	1320	1330	1350	69	1280	1300	1320	1360
21	1600	1600	1600	1600	70	1270	1310	1330	1340
22	1340	1360	1370	1380	71	1450	1480	1500	1510
23	1420	1450	1460	1470	72	1280	1300	1320	1330
24	1500	1550	1580	1590	73	1380	1400	1420	1430
25	1310	1320	1330	1340	74	1300	1330	1350	1360
26	1380	1400	1410	1420	75	1260	1290	1300	1310
27	1600	1600	1600	1600	76	1530	1560	1570	1580
28	1600	1600	1600	1600	77	1250	1310	1350	1370
29	1600	1600	1600	1600	78	1600	1600	1600	1600
30	1460	1470	1490	1500	79	1500	1510	1540	1560
31	1420	1450	1480	1490	80	1490	1500	1520	1530
32	1540	1560	1580	1600	81	1340	1390	1440	1460
33	1600	1600	1600	1600	82	1480	1500	1530	1590
34	1400	1420	1450	1460	83	1300	1340	1380	1390
35	1540	1560	1570	1590	84	1500	1500	1500	1500
36	1500	1550	1580	1600	85	1380	1400	1430	1450
37	1210	1250	1280	1310	86	1500	1500	1500	1500
38	1560	1580	1600	1600	87	1500	1500	1500	1500
39	1450	1460	1480	1490	88	1340	1360	1370	1380
40	1440	1460	1480	1490	89	1250	1270	1290	1300
41	1480	1500	1510	1520	90	1250	1270	1280	1290
42	1390	1400	1420	1430	91	1580	1590	1600	1600
43	1400	1450	1480	1490	92	1380	1410	1460	1470
44	1340	1390	1420	1490	93	1600	1600	1600	1600
45	1540	1560	1570	1590	94	1410	1420	1430	1440
46	1240	1280	1300	1310	95	1280	1310	1340	1350
47	1280	1300	1380	1420	96	1200	1230	1250	1260
48	1600	1600	1600	1600	97	1550	1570	1590	1600
49	1200	1240	1300	1360	98	1600	1600	1600	1600

$$\mathrm{RE} = \frac{Y_{\mathrm{mea}} - Y_{\mathrm{pred}}}{Y_{\mathrm{mea}}} \times 100\% \quad (1)$$

$$\mathrm{MARE} = \frac{\sum_{i=1}^{n} |\mathrm{RE}|}{n} \quad (2)$$

where Y_{meas} and Y_{pred} are the measured and predicted values by the models, and n is the number of model parameters. Afterward, the threshold statistics (TS) is computed based on the outcome of the RE using eq 3.

$$\mathrm{TS} = \frac{Y_{\mathrm{x}}}{n} \quad (3)$$

where TS is the threshold statistics in percentage, and Y_{x} is the number of relative error that is less than the set threshold value. The results obtained for the RE and MARE using the testing and validation data sets are presented in Table 6. The MARE values

https://doi.org/10.1021/acsomega.3c04113
ACS Omega 2023, 8, 39080−39095

Table A2. Proximate Analysis of Coal Samples

	dry basis				dry basis		
sample	ash content %	VM %	fixed carbon %	sample	ash content %	VM %	fixed carbon %
1	31.5	23.5	45	50	25.9	23.8	50.3
2	24.1	24.4	51.5	51	27.2	23	49.8
3	13.1	29.1	57.8	52	30.1	24.2	45.7
4	15.2	26.7	58.1	53	9.8	33.6	56.6
5	16.5	23.4	60.1	54	20.1	24.9	55
6	7.8	30.6	61.6	55	15.4	29.2	55.4
7	10.2	33.5	56.3	56	13.3	29.6	57.1
8	14.9	26.9	58.2	57	13.1	32.8	54.1
9	15.9	27	57.1	58	14.9	25.4	59.7
10	20.1	21.5	58.4	59	7.1	32.5	60.4
11	16.4	27.9	55.7	60	14.2	26.9	58.9
12	17.4	27.1	55.5	61	15.2	27.9	56.9
13	26.9	22	51.1	62	13.6	29.9	565
14	12.2	30.1	57.7	63	11.2	34.6	54.2
15	10.8	33.1	56.1	64	11.2	37	51.8
16	15.1	25.8	59.1	65	22.9	27.7	49.4
17	13.3	26.2	60.5	66	15.6	33.3	51.1
18	11.7	33.7	54.6	67	26	24.3	49.7
19	14	27.3	58.7	68	11	35.2	53.8
20	7.7	33.2	59.1	69	13.2	33.2	53.6
21	17.3	23.9	58.7	70	13.7	31.7	54.6
22	14.2	26.1	59.7	71	14.3	26.3	59.4
23	15.5	24.9	59.6	72	16.4	33.5	50.1
24	8	32.7	59.3	73	15.1	29.4	55.5
25	31.3	24.1	44.6	74	15	9.1	75.9
26	31.9	22.6	45.5	75	16.2	28.5	55.3
27	15.9	22.5	61.6	76	13.9	34.4	51.7
28	15.8	25	59.2	77	13.1	7.6	79.3
29	7.7	32	60.3	78	15.2	23.9	60.9
30	17.2	27.2	55.6	79	10.2	37.1	52.7
31	13.5	26.9	59.6	80	34.4	25.9	39.7
32	17.2	27.2	55.6	81	13.8	23.9	62.3
33	14.4	25.1	60.5	82	40.1	21.3	38.6
34	17.3	26.3	56.4	83	31	24.7	44.3
35	14.2	26.4	59.4	84	15.8	10.1	74.1
36	15.6	24	60.4	85	12.6	29.7	57.7
37	30.2	24.3	45.5	86	20.4	17.1	62.5
38	14.6	24.2	61.2	87	15.8	22.7	61.5
39	8	31.5	60.5	88	12.9	5.9	81.2
40	30.7	21.2	48.1	89	19	8.4	72.6
41	16.8	24.2	59	90	13	7.6	79.4
42	14.8	26	59.2	91	12	9.5	78.5
43	10.3	31.9	57.8	92	13.4	26.2	60.4
44	26.3	25.3	48.4	93	14	25.7	60.3
45	16.6	26.9	56.5	94	16.5	5.6	77.9
46	17.5	25	57.5	95	22.9	6.8	70.3
47	14.4	28.4	57.2	96	22.4	30.2	47.4
48	17.4	26.6	56	97	17.3	19.1	63.6
49	26.9	23	50.1	98	17.2	25.8	57

obtained for ST, HT, FT and DT for the AC-Ash-FC were 0.192674, 0.16645, 0.036896, and 0.235841 respectively for the training, while MARE values of 0.104632, 0.1772735, 0.173453, and 0.207828 were obtained for the validation. For the AC-Ash-VM, the MARE obtained for the ST, HT, FT and DT at the testing phase were 0.089625, 0.116897, 0.197462, and 0.207625 respectively, while 0.28578, 0.085897, 0.121114, and 0.258475 are obtained for the respective temperatures for the validation phase.

Furthermore, for AC-Ash-FC-VM, the obtained MARE values for the training phase for the four temperatures are 0.286617, 0.210525, 0.190938, and 0.104837 respectively while MARE values of 0.166277, 0.2758528, 0.05944, and 0.09412 are obtained for the validation phase for the four temperatures, respectively. Based on the MARE values, it can be said that the HT, AC-Ash-VM model has the lowest MARE values for the training and validation phases and the best for the HT. For the FT, the AC-Ash-FC model seems to be the best though the AC-

https://doi.org/10.1021/acsomega.3c04113
ACS Omega 2023, 8, 39080−39095

Table A3. Ash Analyses of Selected Coal Products

	expressed as constituent in ash %									in coal %	
sample	SiO_2	Al_2O_3	Fe_2O_3	P_2O_5	TiO_2	CaO	MgO	K_2O	Na_2O	SO_3	P_2O_5
1	55.1	24.6	3.58	0.96	1.82	9.01	1.56	0.69	0.20	2.47	0.126
2	45.7	25.1	4.64	1.03	1.88	11.7	2.71	0.66	0.56	4.93	0.103
3	44.5	31.9	5.58	1.54	1.88	7.40	1.78	0.51	0.28	3.71	0.085
4	58.2	30.6	2.56	0.22	1.61	2.91	1.03	0.48	0.20	1.68	0.014
5	46.6	28.8	5.11	1.56	1.53	8.84	2.03	0.46	0.13	4.49	0.110
6	42.3	33.9	4.86	2.07	2.16	8.13	2.01	0.42	0.25	2.74	0.069
7	65.8	25.6	2.82	0.15	1.25	0.53	0.67	1.16	0.12	0.07	0.006
8	51.6	36.2	1.65	0.60	1.71	4.23	0.98	0.54	0.14	1.89	0.038
9	45.4	31.1	19.7	0.77	1.52	0.52	0.14	0.67	0.12	0.12	0.052
10	59.5	34.3	2.75	0.17	1.82	0.15	0.13	0.52	0.07	0.13	0.015
11	46.4	26.8	5.63	2.72	1.43	10.4	1.85	0.50	0.12	3.14	0.189
12	46.2	30.6	2.82	0.86	1.79	9.06	1.85	0.57	0.27	5.45	0.062
13	52.4	29.5	4.85	1.39	1.73	3.85	1.17	0.68	0.09	2.66	0.160
14	58.7	33.5	1.87	0.35	1.64	1.20	0.69	0.62	0.10	1.14	0.018
15	53.8	36.4	5.82	0.25	1.51	0.71	0.30	0.52	0.12	0.44	0.011
16	41.7	28.2	3.40	1.92	1.66	16.1	1.42	0.69	0.07	4.91	0.122
17	62.1	33.1	1.30	0.17	1.92	0.43	0.18	0.46	0.06	0.22	0.010
18	45.7	27.7	3.43	0.39	1.31	9.75	2.94	0.35	0.30	6.85	0.019
19	42.1	33.8	3.11	1.92	1.55	10.0	2.56	0.60	0.42	3.80	0.114
20	41.6	33.8	3.74	2.40	2.08	9.35	1.76	0.71	0.33	3.59	0.079
21	49.5	33.4	1.74	0.34	1.97	6.48	1.94	0.46	0.12	3.37	0.025
22	46.0	31.0	2.50	1.97	1.87	10.5	1.20	0.86	0.10	3.41	0.119
23	49.3	34.4	2.47	0.88	1.76	6.15	1.04	0.43	0.10	2.66	0.058
24	45.6	35.9	2.50	1.41	2.29	6.68	0.97	0.71	0.16	2.58	0.048
25	47.4	28.8	5.22	0.67	1.60	8.66	1.84	0.81	0.16	4.31	0.088
26	50.1	30.5	5.26	0.93	1.96	5.81	1.67	0.72	0.20	2.34	0.125
27	48.1	36.3	2.89	1.71	1.74	5.00	0.80	0.52	0.11	2.08	0.116
28	47.8	37.6	1.92	2.09	1.86	5.00	0.69	0.58	0.13	1.96	0.140
29	45.8	39.9	2.63	1.19	2.35	4.73	0.60	0.63	0.15	1.80	0.039
30	47.3	34.3	1.89	0.50	1.84	7.94	1.91	0.46	0.10	3.49	0.036
31	43.3	36.0	2.29	1.99	1.80	7.75	1.64	0.55	0.21	3.10	0.114
32	52.3	33.8	2.55	0.42	1.87	5.21	1.33	0.50	0.11	1.80	0.030
33	49.1	38.0	2.09	1.53	2.42	3.87	0.59	0.54	0.10	1.77	0.093
34	47.7	35.3	1.90	0.44	1.96	7.26	1.85	0.45	0.11	3.01	0.032
35	47.1	36.2	3.22	4.26	1.18	5.72	0.16	0.22	0.09	0.12	0.255
36	42.6	36.0	2.33	0.71	2.08	8.15	1.98	0.84	0.71	4.54	0.046
37	53.4	28.0	4.14	0.71	1.57	6.30	1.72	1.04	0.50	2.27	0.090
38	56.3	32.5	2.65	1.03	2.17	2.17	0.61	0.62	0.09	1.11	0.064
39	45.9	33.3	3.40	1.53	1.87	6.93	1.86	0.72	0.22	2.99	0.052
40	62.3	20.8	4.43	0.17	1.62	2.90	1.08	0.64	0.49	1.77	0.022
41	45.1	35.4	1.92	0.52	2.36	8.52	0.85	1.29	0.08	2.59	0.036
42	44.6	32.4	2.90	2.34	1.72	8.90	2.54	0.44	0.12	2.46	0.143
43	51.0	31.0	2.52	2.51	1.45	5.14	1.64	0.94	0.32	1.58	0.108
44	58.6	25.9	3.64	0.49	1.40	3.94	1.74	0.85	0.11	2.69	0.054
45	56.0	30.9	2.29	0.34	1.81	3.68	1.13	0.34	0.17	2.58	0.024
46	48.8	23.7	10.7	0.62	1.33	6.49	2.47	0.40	0.19	4.79	0.046
47	47.4	31.9	3.33	1.41	2.00	7.75	1.93	0.58	0.18	2.98	0.086
48	61.3	33.9	0.76	0.17	2.55	0.19	0.04	0.56	0.05	0.02	0.013
49	52.1	23.0	6.33	0.72	1.55	8.13	2.35	0.59	0.45	4.56	0.081
50	54.8	25.6	3.35	0.74	1.92	6.18	1.98	0.90	0.40	3.99	0.080
51	52.7	27.3	2.13	0.73	1.55	7.46	2.74	0.58	0.45	4.07	0.083
52	56.6	22.22	5.39	0.57	1.21	5.31	2.49	1.36	0.69	2.48	0.070
53	41.7	32.4	3.63	1.41	1.87	10.3	2.96	0.61	0.60	4.14	0.058
54	47.4	30.2	1.83	1.19	1.64	8.05	3.24	0.59	0.50	3.67	0.100
55	44.3	27.4	2.93	1.99	1.41	16.1	1.86	0.42	0.28	2.99	0.129
56	49.33	26.5	2.22	1.62	1.74	9.58	2.03	0.60	0.16	4.31	0.091
57	62.9	25.9	2.36	0.42	1.12	2.57	0.95	1.33	0.16	4.31	0.023
58	47.0	32.7	3.14	1.82	1.75	7.54	1.46	0.48	0.20	2.38	0.115
59	39.7	33.9	3.24	2.33	2.24	9.06	2.07	0.61	0.36	5.03	— *

https://doi.org/10.1021/acsomega.3c04113
ACS Omega 2023, 8, 39080−39095

Table A3. continued

	expressed as constituent in ash %									in coal %	
sample	SiO_2	Al_2O_3	Fe_2O_3	P_2O_5	TiO_2	CaO	MgO	K_2O	Na_2O	SO_3	P_2O_5
60	50.7	26.2	2.99	2.60	1.58	8.40	1.31	0.46	0.18	3.58	0.157
61	36.9	29.4	8.83	2.11	1.19	11.5	2.74	0.48	0.25	5.01	0.136
62	60.8	32.4	1.32	0.44	1.57	0.85	0.32	0.43	0.10	0.32	0.025
63	61.6	32.5	1.22	0.18	1.50	0.56	0.27	0.40	0.10	0.34	0.008
64	58.1	31.2	4.73	0.21	1.39	1.37	0.52	0.55	0.30	1.36	0.010
65	61.9	26.5	8.20	0.32	1.19	0.56	0.23	0.39	0.08	0.43	0.031
66	54.3	21.9	10.6	1.37	1.09	5.90	0.61	0.45	0.12	3.51	0.091
67	40.6	33.9	6.87	1.52	1.84	8.17	3.01	0.42	0.15	3.21	0.165
68	46.7	27.8	7.36	0.29	1.34	6.44	2.13	0.53	0.54	5.68	0.013
69	51.8	24.8	9.47	0.42	1.55	4.92	1.31	0.72	0.20	3.94	0.023
70	51.8	24.8	9.47	0.42	1.55	4.92	1.31	0.72	0.20	3.94	0.023
71	53.6	29.1	1.90	0.51	1.63	6.13	2.43	0.35	0.15	3.40	0.030
72	57.4	22.5	7.09	1.33	1.09	5.84	0.60	0.49	0.14	3.47	0.092
73	51.0	30.9	2.64	0.62	1.55	6.54	1.92	0.60	0.16	3.93	0.040
74	52.0	26.7	6.96	0.23	1.40	4.50	2.33	1.03	1.12	2.56	0.015
75	45.2	21.0	11.1	0.37	1.14	11.3	1.87	0.42	0.60	5.56	0.025
76	51.1	31.5	8.71	0.20	1.07	3.19	1.06	0.59	0.15	2.00	0.012
77	45.9	30.6	9.49	1.69	1.33	4.61	1.44	0.43	0.91	3.54	0.095
78	47.2	38.6	1.00	1.02	2.16	4.60	1.14	0.41	0.16	2.83	0.066
79	71.3	17.5	4.68	0.22	1.59	0.93	0.48	0.79	0.12	0.64	0.010
80	56.3	26.3	7.52	0.70	1.19	3.08	0.77	0.72	0.17	1.39	0.103
81	59.0	25.1	5.05	0.58	1.45	3.32	1.39	1.37	0.67	2.06	0.035
82	54.1	31.1	3.28	0.35	1.63	4.74	0.94	0.40	0.24	2.25	0.058
83	54.0	28.7	3.42	0.31	1.76	6.22	1.24	0.49	0.42	3.12	0.039
84	49.1	31.4	5.79	1.20	1.43	4.10	0.71	1.99	0.87	1.98	0.081
85	48.3	30.5	6.55	0.64	1.25	5.82	1.05	1.87	0.91	2.55	0.035
86	47.6	28.9	6.05	0.70	1.57	5.63	1.43	1.51	1.37	3.59	0.061
87	45.6	24.3	8.68	0.73	1.40	8.76	2.47	1.51	0.81	5.40	0.049
88	53.2	27.4	7.42	0.30	1.62	1.87	1.17	2.08	2.84	0.88	0.016
89	47.9	25.9	4.63	0.98	1.29	8.54	1.97	1.33	1.80	4.00	0.079
90	50.0	26.0	4.89	1.77	1.21	8.03	1.43	1.50	1.76	2.83	0.098
91	53.1	32.3	6.16	0.32	1.56	0.96	0.83	2.35	1.04	0.76	0.016
92	59,4	24.5	6.40	0.20	1.24	2.27	1.07	1.59	1.21	1.99	0.012
93	53.6	32.5	6.10	0.17	1.75	1.19	0.69	1.69	0.97	1.30	0.010
94	47.6	29.1	13.1	0.88	1.77	1.53	1.08	2.35	0.52	0.62	0.028
95	52.3	28.1	10.1	0.54	1.31	2.03	0.88	2.92	0.33	1.33	0.038
96	46.0	24.5	8.78	0.26	1.06	8.41	1.26	0.56	0.22	8.06	0.024
97	55.6	28.7	4.23	0.46	2.04	1.40	0.72	1.93	1.17	1.81	0.034
98	50.6	35.4	3.09	0.86	2.21	3.59	0.95	1.33	0.16	1.23	0.063

Ash-FC-VM model also shows good performance most importantly at the validation phase. For the DT, the AC-Ash-FC-VM model outperformed other combinations of parameters and therefore the best. The ST has not been clearly established with MARE, and the AC-Ash-VM model has the least MARE value at the testing phase and the least at the validation. Hence, this will be better estimated with the TS. The threshold value is set at 0.2%, i.e., the percentage of RE that is less than or equal to 0.2%. The values are shown in Table 7. For the HT, AC-Ash-VM is the most favored while for the FT, AC-Ash-FC is the best. For the DT, AC-Ash-FC-VM is the best. However, for the ST, AC-Ash-VM could be chosen, but any of the three combinations can also be used.

4. CONCLUSIONS

In this study, a total of 98 coal samples from the South African Coalfields were collected and investigated. Following the acquisition of coal characteristics and subsequent AFTs, the most suitable model among the developed models was proposed to predict the AFTs of South African coal. Based on the relationship between the coal properties and the AFTs of coal, an ANN model termed the MISO-ANN was used to predict the AFTs. This study indicates that a combination of parameters such as AC-Ash-VM is the most favored for the prediction of HT, AC-Ash-FC is the best for the prediction of FT, and AC-Ash-FC-VM is the best for the prediction of DT. However, for the ST, AC-Ash-VM could be chosen but any of the three combinations can be used. This finding demonstrates that the prediction results obtained by using the proposed method are accurate. As a result, the optimized ANN is considered as a highly successful way in predicting coal AFT, and it could be applied in future industrial applications. The study demonstrates that ANNs are capable of accurately predicting the AFTs in coal from proximate analysis and ash chemistry.

APPENDIX A

The details of the adopted data set from the experimental outcomes are presented in Tables A1−A3.

https://doi.org/10.1021/acsomega.3c04113
ACS Omega 2023, 8, 39080−39095

AUTHOR INFORMATION

Corresponding Author

Moshood Onifade − *Department of Mining Engineering and Mine Surveying, University of Johannesburg, Doornfontein 2028, South Africa;* orcid.org/0000-0001-9933-266X; Phone: +27740284611; Email: lonifade4@gmail.com

Authors

Abiodun Ismail Lawal − *Department of Mining Engineering, Federal University of Technology, Akure 340110, Nigeria*

Samson Oluwaseyi Bada − *DSI/NRF Clean Coal Technology Research Group, School of Chemical and Metallurgical Engineering, Faculty of Engineering and the Built Environment, University of the Witwatersrand, WITS, Johannesburg 2050, South Africa;* orcid.org/0000-0002-1079-3492

Amtenge Penda Shivute − *Department of Civil and Mining Engineering, University of Namibia, Windhoek 13301, Namibia*

Complete contact information is available at: https://pubs.acs.org/10.1021/acsomega.3c04113

Notes

The authors declare no competing financial interest.

ACKNOWLEDGMENTS

The authors gratefully acknowledge with thanks the financial support of the National Research Foundation (NRF) of South Africa's SARChI Clean Coal Technology Grant. Opinions, findings, and conclusions expressed are those of the authors and the NRF accepts no liability whatsoever in this regard.

REFERENCES

(1) Van Dyk, J.; Keyser, M. Influence of discard mineral matter on slag − liquid formation and ash melting properties of coal − A FACTSAGETM simulation study. *Fuel* **2014**, *116*, 834−840.

(2) Li, K.; Khanna, R.; Zhang, J.; Barati, M.; Liu, Z.; Xu, T.; Yang, T.; Sahajwalla, V. Comprehensive investigation of various structural features of bituminous coals using advanced analytical techniques. *Energy Fuel* **2015**, *29* (11), 7178−7189.

(3) Wang, G.; Zhang, J.; Shao, J.; Liu, Z.; Zhang, G.; Xu, T.; Guo, J.; Wang, H.; Xu, R.; Lin, H. Thermal behaviour and kinetic analysis of co-combustion of waste biomass/low rank coal blends. *Energy Convers. Manag.* **2016**, *124*, 414−426.

(4) Wang, G.; Zhang, J.; Huang, X.; Liang, X.; Ning, X.; Li, R. Co-gasification of petroleum coke biomass blended char with steam at temperatures of 1173−1373 K. *Appl. Therm. Eng.* **2018**, *137*, 678−688.

(5) Liu, B.; He, Q.; Jiang, Z.; Xu, R.; Hu, B. Relationship between coal ash composition and ash fusion temperatures. *Fuel* **2013**, *105*, 293−300.

(6) Yu, L.; Wang, L.; Li, P. Study on prediction models of biomass ash softening temperature based on ash composition. *J. Energy Inst.* **2014**, *87* (3), 215−219.

(7) Lawal, A. I.; Onifade, M.; Bada, S.; Shivute, A. P.; Abdulsalam, J. Prediction of thermal coal ash behaviour of South African coal: A comparative applications of ANN, GPR, and SVR. *Nat. Res. Res.* **2023**, *32* (3), 1399−1413.

(8) Chakravarty, S.; Mohanty, A.; Banerjee, A.; Tripathy, R.; Mandal, G. K.; Basariya, M. R.; Sharma, M. Composition, mineral matter characteristics and ash fusion behaviour of some Indian coals. *Fuel* **2015**, *150*, 96−101.

(9) Yan, T.; Bai, J.; Kong, L.; Bai, Z.; Li, W.; Xu, J. Effect of SiO_2/Al_2O_3 on fusion behaviour of coal ash at high temperature. *Fuel* **2017**, *193*, 275−283.

(10) Mao, Y.; Jin, Y.; Li, K.; Bi, J.; Li, J.; Xin, F. Sintering Characteristic in Catalytic Gasification of China Inner Mongolia Bituminous Coal Ash. *Energy Fuels* **2016**, *30*, 3975−3985.

(11) Liu, C.; Bai, Y.; Yan, L.; Zuo, Y.; Wang, Y.; Li, F. Impact of alkaline oxide on coal ash fusion temperature. *Int. J. Oil Gas Coal Technol.* **2014**, *8*, 79.

(12) Wei, B.; Wang, X.; Tan, H.; Zhang, L.; Wang, Y.; Wang, Z. Effect of silicon-aluminium additives on ash fusion and ash mineral conversion of Xinjiang high-sodium coal. *Fuel* **2016**, *181*, 1224−1229.

(13) Song, W. J.; Tang, L. H.; Zhu, X. D.; Wu, Y. Q.; Zhu, Z. B.; Koyama, S. Effect of coal ash composition on ash fusion temperatures. *Energy Fuel* **2010**, *24* (1), 182−189.

(14) ASTM D - 87: Standard Test Method for Fusibility of Coal and Coke Ash. 1985, Annual Book of Standards.

(15) Li, Q.; Zhang, Y.; Meng, A.; Li, L.; Li, G. Study on ash fusion temperature using original and simulated biomass ashes. *Fuel Process. Technol.* **2013**, *107*, 107−112.

(16) Luan, C.; You, C.; Zhang, D. An experimental investigation into the characteristics and deposition mechanism of high-viscosity coal ash. *Fuel* **2014**, *119*, 14−20.

(17) Bilen, M. Ash melting behaviour of some low-grade Turkish coals and some imported steam coals. *Combust. Theory Modell.* **2019**, *23* (6), 1105−1118.

(18) Seggiani, M.; Pannocchia, G. Prediction of coal ash thermal properties using partial least-squares regression. *Ind. Eng. Chem. Res.* **2003**, *42*, 4919−4926.

(19) Seggiani, M. Empirical correlations of the ash fusion temperatures and temperature of critical viscosity for coal and biomass ashes. *Fuel* **1999**, *78*, 1121−1125.

(20) Van Dyk, J. C.; Keyser, M. J.; Van Zyl, J. W. Suitability of feedstocks for the Sasol−Lurgi fixed bed dry bottom gasification process. In *Gasification Technology Conference*; Gasification Technologies Council: Arlington, 2001, Paper 10−18.

(21) Ozbayoglu, G.; Ozbayoglu, M. E. A new approach for the prediction of ash fusion temperatures: a case study using Turkish Lignites. *Fuel* **2006**, *85*, 545−562.

(22) Wall, T. F.; Creelman, R. A.; Gupta, R. P.; Coin, C.; Lowe, A. Coal ash fusion temperatures-new characterization techniques, and implications for slagging and fouling. *Prog. Energy Combust. Sci.* **1998**, *24*, 345−353.

(23) Hurst, H. J.; Novak, F.; Patterson, J. H. Phase diagram approach to the fluxing effect of additions of CaCO3 on Australian coal ashes. *Energy Fuels* **1996**, *10*, 1215−1219.

(24) Tambe, S. S.; Naniwadekar, M.; Tiwary, S.; Mukherjee, A.; Das, T. B. Prediction of coal ash fusion temperatures using computational intelligence based models. *Int. J. Coal Sci. Technol.* **2018**, *5* (4), 486−507.

(25) Xiao, H.; Chen, Y.; Dou, C.; Ru, Y.; Cai, L.; Zhang, C.; Kang, Z.; Sun, B. Prediction of ash-deformation temperature based on grey-wolf algorithm and support-vector machine. *Fuel* **2019**, *241*, 304−310.

(26) Tillman, D.; Duong, D. Managing slagging at Monroe power plant using on-line coal analysis and fuel blending. *Fuel Process. Technol.* **2007**, *88* (11−12), 1094−1098.

(27) Holubcik, M.; Jandacka, J.; Malcho, M. Ash melting temperature prediction from chemical composition of biomass ash. *Holist. Approach Environ.* **2015**, *5* (3), 119−125.

(28) Bilen, M.; Kizgut, S. 2016 Ash melting behaviour with respect to VM content of coal. In *XVIII International Coal Preparation Congress*, Litvinenko, V., ed.; Springer: Cham, 2016.

(29) Wang, L.; Guangwei, W.; Xiaojun, N.; Jianliang, Z.; Yanjiang, L.; Chunhe, J.; Nan, Z. Application of BP neural network to the prediction of coal ash melting characteristic temperature. *Fuel* **2020**, *260*, No. 116324.

(30) ASTM, D-3682−13. Standard Test Methods for ash in the analysis sample of coal and coke from coal, ASTM, International, West Conchohocken, PA, www.astm.org.

(31) ASTM, D5142. Standard Test Methods for Proximate Analysis of the Analysis Sample of Coal and Coke by Instrumental Procedures.

(32) Bui, X.-N.; Nguyen, H.; Le, A. H.; Bac, B. H.; Hoan, D. N. Prediction of Blast-induced Air Over-pressure in Open-Pit Mine: Assessment of Different Artificial Intelligence Techniques. *Nat. Resour. Res.* **2020**, *29*, 571 DOI: 10.1007/s11053-019-09461-0.
(33) Tang, L.; Na, S.-H. Comparison of machine learning methods for ground settlement prediction with different tunnelling datasets. *J. Rock Mech. Geotech. Eng.* **2021**, *13* (6), 1274−1289.
(34) Lawal, A. I.; Kwon, S. Development of mathematically motivated hybrid soft computing models for improved predictions of ultimate bearing capacity of shallow foundations. *J. Rock Mech. Geotech. Eng.* **2023**, *15* (3), 747−759.
(35) Onifade, M.; Lawal, A. I.; Abdulsalam, J.; Genc, B.; Bada, S.; Said, K. O.; Gbadamosi, A. R. Development of multiple soft computing models for estimating organic and inorganic constituents in coal. *Int. J. Mining Sci. Technol.* **2021**, *31* (3), 483−494.
(36) Abdullah, Z.; Ahmad, Z.; Aziz, N. Multiple input-single output (MISO) feed forward artificial neural network (fann) models for pilot plant binary distillation column. In *2011 Sixth International Conference on Bio-Inspired Computing: Theories and Applications*, 2011.
(37) Abdulsalam, J.; Lawal, A. I.; Setsepu, R. L.; Onifade, M.; Bada, S. Application of gene expression programming, artificial neural network and multilinear regression in predicting hydrochar physicochemical properties. *Bioresour. Bioprocess.* **2020**, *7*, 62.
(38) Akinwekomi, A. D.; Lawal, A. I. Neural network-based model for predicting particle size of AZ61 powder during high energy mechanical milling. *Neural Comput. Appl.* **2021**, *33*, 17611−17619.
(39) Willmott, C. J.; Matsuura, K. Advantages of the Mean Absolute Error (MAE) Over the Root Mean Square Error (RMSE) in Assessing Average Model Performance. *Clim. Res.* **2005**, *30* (1), 79−82.
(40) Jain, A.; Varshney, A. K.; Joshi, U. C. Short term water demand forecast modelling at IIT Kanpur using artificial neural networks. *Water Res. Manag.* **2001**, *15* (5), 299−321.

https://doi.org/10.1021/acsomega.3c04113
ACS Omega 2023, 8, 39080−39095